Angewandte Chemie

DOI: 10.1002/ange.201108098

Nanostructures

Synthesis of Hollow $Cd_xZn_{1-x}Se$ Nanoframes through the Selective Cation Exchange of Inorganic–Organic Hybrid ZnSe–Amine Nanoflakes with Cadmium Ions[**]

*Xuan Wu, Yifu Yu, Yang Liu, You Xu, Cuibo Liu, and Bin Zhang**

Novel applications of nanostructures in catalysis, electronics, photonics, and bionanotechnology[1] are driving the exploration of synthetic approaches to control and manipulate the morphology and chemical composition of nanostructures.[2–5] Among these nanomaterials, hollow skeleton-like structures involving nanorings,[3] nanoskeletons,[4] and nanoframes[5] have attracted increasing interest owing to their unique structures, interesting properties, which are different from their solid counterparts, and promising applications in different fields.[3–5] In recent years, hollow skeleton-like or frame-like Au, Co, Fe, Cu_2O, Fe_2O_3, ZnO nanostructures have been successfully fabricated by using many advanced methods including self-assembly or oriented attachment of nanocrystals, template-assisted chemical etching, and self-coiling of nanobelts. However, with present methods the synthesis of frame-shaped semiconductors of controlled composition is a great challenge. Thus, it should be of great interest to develop a facile approach to generate frame-like hollow materials with adjustable composition, because the properties of these materials are strongly dependent on their composition.[6]

Since Alivisatos and coworkers discovered the cation-exchange reaction in nanocrystals,[7] the cation-exchange reaction has received growing attention as an effective way to modulate the composition, the structure, and the properties of nanomaterials.[8–14] For instance, a partial cation-exchange reaction was adopted to create semiconductor superlattice structures in nanorods.[8] Chalcogenide gels and metal phosphides and sulfides were successfully generated by the ion-exchange reaction of corresponding nanostructures by Brock's group.[9] Dorn et al. developed an in situ electric measuring method to monitor the exchange process of nanowires.[10] Our recent study demonstrated that the vapor-phase cation-exchange reaction of CdS with organic zinc could generate one-dimensional nanostructures with adjustable composition, morphology, and optical properties.[11] Interestingly, the selectivity of facet reactivity was also observed in the case of the cation-exchange reactions of CdS nanorods and octapod-shaped CdS nanocrystals.[12] At present, research efforts mainly focused on modulating the composition, structure, and properties of solid inorganic nanocrystals or one-dimensional nanostructures, while preserving their size and shape. Recently, we adopted the inorganic–organic hybrid sheets as starting materials and described a facile cation-exchange strategy to fabricate single-crystal-like porous nanosheets.[13] Although these advances have been achieved, the development of selective cation-exchange reactions to synthesize frame-like nanostructures, especially with adjustable composition, is still in its infancy.

Herein, we report a facile and effective protocol to prepare $Cd_xZn_{1-x}Se$ nanoframes through the selective cation-exchange reaction of unpurified inorganic–organic ZnSe–amine nanosheets with Cd^{2+} ions (see Figure 1 a). We show that $Cd_xZn_{1-x}Se$ nanoframes with adjustable composition are accessible by varying the relative ratio of hybrid precursors to cations in this approach. Moreover, the selective cation-exchange strategy of hybrid nanosheets is suitable for fabricating other frame-like nanostructures. Furthermore, we demonstrate that the as-prepared $Cd_{0.33}Zn_{0.67}Se$ nanoframes are highly active for photocatalytic H_2 evolution from water splitting. The composition of hollow $Cd_xZn_{1-x}Se$ nanoframes has exerted an important influence on their photocatalytic activities.

The unpurified ZnSe–DETA nanosheets (DETA = diethylenetriamine) were first prepared using a modified amine-assisted solvothermal method,[15] and were then reacted with different concentrations of Cd^{2+} ions to obtain $Cd_xZn_{1-x}Se$ nanoframes (see the Supporting Information). The ZnSe–DETA nanosheets were firstly examined using scanning electron microscopy (SEM) and energy-dispersive X-ray spectroscopy (EDX). SEM images (Figure 1 b,c) clearly demonstrate that ZnSe–DETA nanosheets were successfully synthesized in high yields. The typical X-ray diffraction (XRD) pattern of the as-prepared hybrid precursors shown in Figure 1 f is identical to that of the reported $ZnSe(DETA)_{0.5}$ nanobelts,[15] thus suggesting that the composition of the as-prepared hybrid nanosheets is $ZnSe(DETA)_{0.5}$ (named ZnSe–DETA here). When ZnSe–DETA nanosheets exchange with an appropriate amount of Cd^{2+} ions at elevated temperature, the solid sheets become hollow frame-like ones with a skeleton size of 30–40 nm (Figure 1 d,e). The FTIR spectra shown in Figure 1 g also confirm that the hybrid precursors can be successfully transformed into inorganic materials. The composition of hollow $Cd_xZn_{1-x}Se$ nanoframes

---

[*] X. Wu, Y. Yu, Y. Liu, Y. Xu, C. Liu, Prof. Dr. B. Zhang
Department of Chemistry, School of Science, Tianjin University
Tianjin 300072 (P. R. China)
E-mail: bzhang@tju.edu.cn

[**] This work was financially supported by the National Natural Science Foundation of China (20901057 and 11074185), National Basic Research Program of China (2009CB939901), the Tianjin Natural Science Foundation (10JCYBJC01800), State Key laboratory of Crystal Material at Shandong University (KF0910), and Innovation Foundation of Tianjin University.

Supporting information for this article is available on the WWW under http://dx.doi.org/10.1002/anie.201108098.

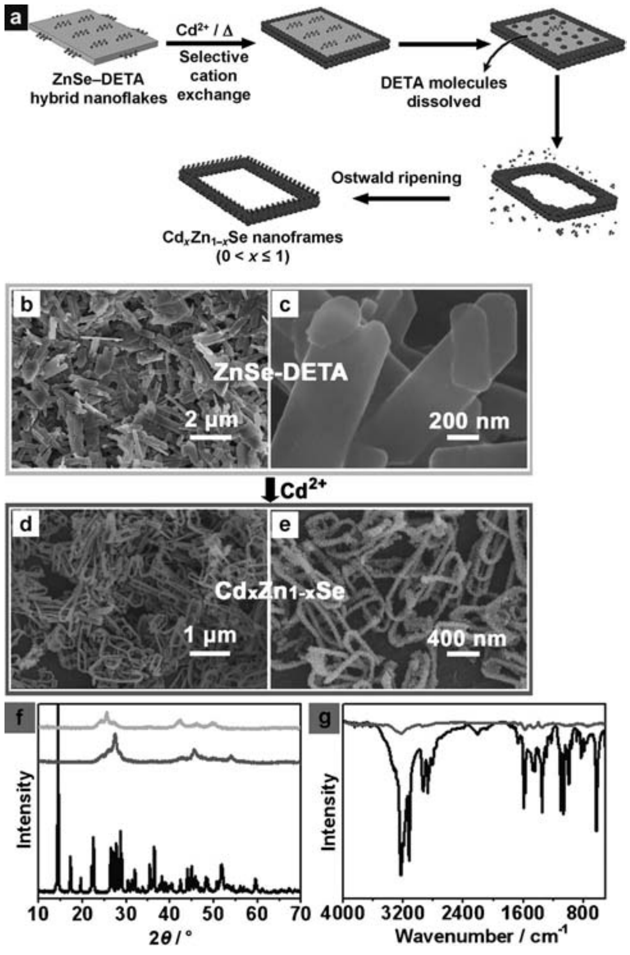

Figure 1. a) Scheme illustrating the synthesis of composition-tunable $Cd_xZn_{1-x}Se$ nanoframes through the selective cation-exchange reaction of the unpurified inorganic–organic ZnSe–DETA hybrid sheets with Cd^{2+} ions at 150 °C. b, c) SEM images of the ZnSe–DETA nanoflakes. d, e) Typical SEM images of hollow $Cd_{0.33}Zn_{0.67}Se$ nanoframes prepared by the selective cation-exchange reaction of the ZnSe–DETA nanoflakes. f) XRD patterns of ZnSe–DETA nanosheets (black, lowest trace), $Cd_{0.33}Zn_{0.67}Se$ nanoframes (dark gray, middle trace), and CdSe (light gray, upper trace). g) FTIR spectra of ZnSe–DETA nanosheets (black, lower trace) and $Cd_{0.33}Zn_{0.67}Se$ nanoframes (dark gray, upper trace).

can be modulated by varying the ratio of the starting hybrid sheets to metal cations. For instance, when the ratio of ZnSe–DETA to Cd^{2+} is 3:1, the products are $Cd_{0.33}Zn_{0.67}Se$ nanoframes, as displayed in the SEM images (Figure 1 d, e), the associated EDX spectrum (see Figure S1 in the Supporting Information), and the inductively coupled plasma emission spectrograph (ICP). By controlling the molar ratio of the starting hybrid materials to cadmium cations, $Cd_{0.25}Zn_{0.75}Se$, $Cd_{0.5}Zn_{0.5}Se$, $Cd_{0.87}Zn_{0.13}Se$, and CdSe hollow nanoframes can be generated (see Figure S1 and Table S1 in the Supporting Information). But, when the hybrid precursors react with an excess of Cd^{2+} ions, the completely exchanged products are porous network-like CdSe flakes rather than frame-shaped CdSe (see Figure S2 in the Supporting Information). This finding indicates that the relative initial cation concentration is important for the formation of nanoframes through selective cation exchange. We find that the final products of one-step partial exchange reactions of hybrid ZnSe–DETA with cadmium ions are $Cd_xZn_{1-x}Se$ nanoframes $(0 < x \le 1)$ when the molar ratio of $CdCl_2$ to ZnSe–DETA is lower than 1.2. These results suggest that $Cd_xZn_{1-x}Se$ nanoframes with a controlled composition can be successfully synthesized by such selective cation-exchange reactions of the inorganic–organic hybrid nanosheets.

The cation-exchange-induced transformations were further characterized using transmission electron microscopy (TEM), high-resolution TEM (HRTEM), and electron energy loss spectroscopy (EELS). The TEM image of ZnSe–DETA hybrid nanosheets (Figure 2 a) shows the flake-like solid morphology of the hybrid precursors. The typical TEM image of the $Cd_{0.33}Zn_{0.67}Se$ nanoframes displayed in Figure 2 b shows that the nanoframes with a skeleton size of approximately 40 nm are obtained in high yield. High-magnification TEM image (the inset in Figure 2 c) and HRTEM image (Figure 2 c) show that the skeletons in hollow $Cd_{0.33}Zn_{0.67}Se$ nanoframes are composed of single-crystalline nanorods with a size of 8–20 nm. Furthermore, it was found that other $Cd_xZn_{1-x}Se$ nanoframes with different composition $(0 < x \le 1)$ possess a shape similar to that of $Cd_{0.33}Zn_{0.67}Se$ (see Figure S1 in the Supporting Information). EELS elemental mapping images (Figure 2 d) imply that the nanoframes are composed of Cd, Zn, and Se. These results demonstrate that the composition of the highly crystalline hollow $Cd_xZn_{1-x}Se$ nanoframes can be successfully adjusted by changing the relative ratio of hybrid precursors to cations in the current approach.

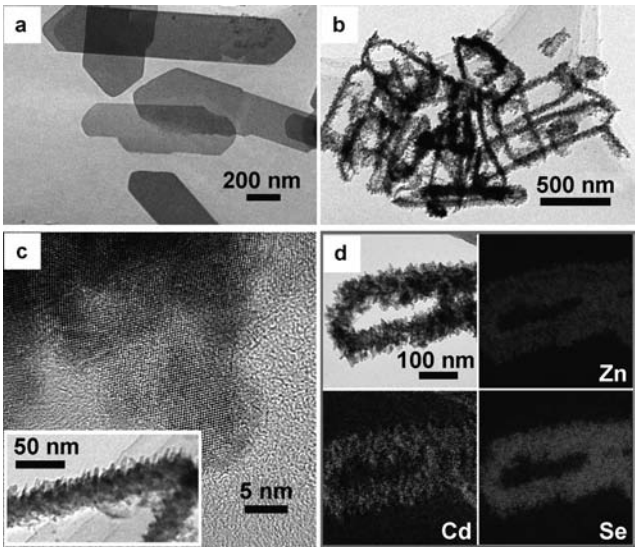

Figure 2. a) TEM image of the ZnSe–DETA hybrid nanosheets; b) TEM image of the $Cd_{0.33}Zn_{0.67}Se$ nanoframes; c) HRTEM image and high-magnification TEM (inset) of the $Cd_{0.33}Zn_{0.67}Se$ nanoframes; d) EELS elemental mapping images of $Cd_{0.33}Zn_{0.67}Se$ nanoframes. The $Cd_{0.33}Zn_{0.67}Se$ nanoframes were prepared through the selective cation exchange reaction of the ZnSe–DETA hybrid sheets with Cd^{2+}.

To clarify the formation mechanism of hollow nanoframes prepared by the selective cation-exchange method, SEM,

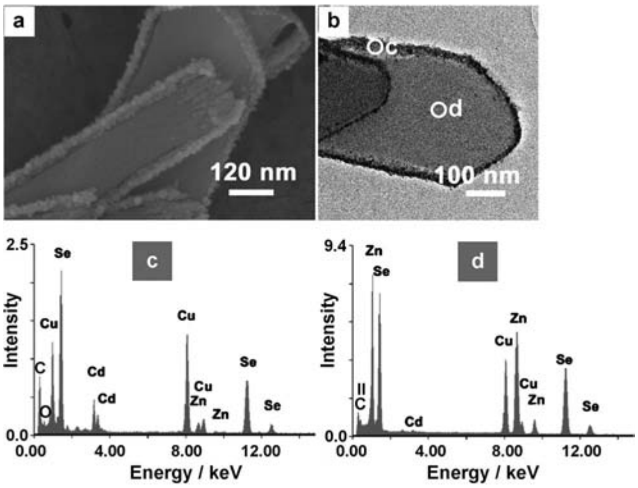

Figure 3. a) Typical SEM image, b) TEM image, and c, d) the point-scan EDX spectra of the intermediates collected after the cation exchange proceeded for 0.5 h, suggesting the selectivity of the cation-exchange reaction of ZnSe–DETA with Cd^{2+}. The circles in (b) indicate the positions where the EDX spectra for (c) and (d) were obtained.

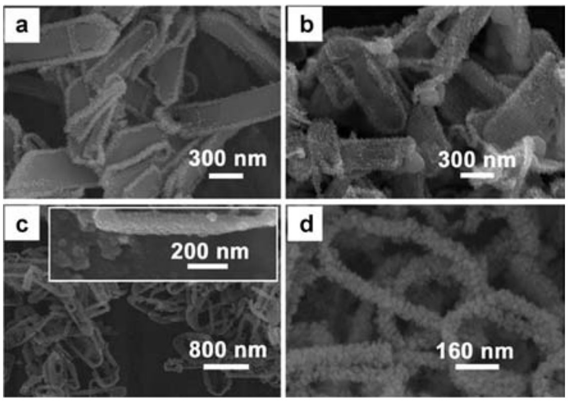

Figure 4. SEM images of the intermediates collected after the selective cation-exchange reaction proceeded for different times: a) 2 h, b) 3 h, c) 4 h, d) 5 h.

TEM, and EDX were used to characterize the intermediates collected at different reaction stages. When the exchange reaction of the unpurified ZnSe–DETA nanosheets with Cd^{2+} ions proceeds for 0.5 h, the edges of the sheets become rough, while their middle parts are still smooth (Figure 3 a, b), indicating that the edges of the hybrid sheets are more reactive than the middle parts of the sheets. The point-scan EDX spectra of the edge and the middle (Figure 3 c, d) reveal that most of the zinc ions in the edges of ZnSe–DETA nanosheets have been exchanged with Cd^{2+}, while Zn^{2+} ions in the middle parts of the nanosheets are almost not exchanged with Cd^{2+} ions, thus confirming the cation-exchange reaction is selective for the unpurified inorganic–organic hybrid nanosheets. But, when ZnSe–DETA nanoflakes are rinsed for several times and then exchanged with Cd^{2+} ions, the exchange reaction occurs uniformly for the whole sheets to produce nanoporous $Cd_xZn_{1-x}Se$ nanosheets (see Figure S3 in the Supporting Information), as observed in the formation process of porous $Cd_xZn_{1-x}Se$ and $Cd_xZn_{1-x}S$ nanosheets.[13] This observation implies that the selectivity in cation exchange of unpurified hybrid nanosheets does not originate from the differences in crystal planes of ZnSe–DETA; these differences are commonly described for the selective chemical etching of inorganic nanocrystals.[2,4,16] Therefore, it is reasonable to speculate that the cation-exchange selectivity of unpurified hybrid nanosheets should be attributed to the fact that DETA molecules are adsorbed more easily onto the top/bottom surface of ZnSe–DETA sheets than onto the edges of the sheets, thus making the exchange reaction more favorable for the edge regions of ZnSe–DETA sheets. When the exchange reaction proceeds for two hours, the edges of the nanosheets become rougher (Figure 4 a). Some nanoparticles appear after three hours of exchange reaction (Figure 4 b), thus suggesting that zinc ions in the middle parts exchanged with Cd^{2+}, because the DETA molecules adsorbed on the surface are slowly dissolved into aqueous solution. The prolonged exchange reaction and the slow dissolution of DETA in water make the middle area of the sheets break into small particles, and the edges become bigger and rougher (Figure 4 c). These small nanoparticles may dissolve and regrow on bigger frames (Figure 4 d) through the typical Ostwald ripening mechanism.[17] This process finally leads to the formation of $Cd_xZn_{1-x}Se$ nanoframes with a skeleton composed of branch-like nanorods (Figure 1 d, e and Figure 2 b). On the basis of these results above, we propose the transformation mechanism of ZnSe–DETA sheets into $Cd_xZn_{1-x}Se$ nanoframes involving the selective cation-exchange reaction of hybrid sheets, the dissolution of DETA, and the following Ostwald ripening process, as displayed in Figure 1 a.

At room temperature, the hybrid nanosheets can also evolve into frame-like $Cd_xZn_{1-x}Se$ nanoframes, but the complete reaction requires longer time (over four weeks; see Figure S4 in the Supporting Information). This finding suggests that the selective exchange reaction between the hybrid nanosheets and the Cd^{2+} ions is dependent on the reaction temperature. Furthermore, as discussed above, when the ratio of Cd^{2+} ions to ZnSe–DETA is higher than 1.2:1, the samples are porous sheets rather than nanoframes (see Figure S2 in the Supporting Information). This observation reveals that the high concentration of Cd^{2+} ions can destroy the selective cation-exchange reaction, which is important for the formation of nanoframes.

This selective cation-exchange strategy presented herein can be broadened to the synthesis of nanoframes of other metal selenides and sulfides. For instance, when unpurified ZnS–DETA nanosheets are used as the starting materials for a cation-exchange reaction with Cd^{2+} ions, $Cd_xZn_{1-x}S$ nanoframes can be also generated (see Figure S5 in the Supporting Information). This additional work indicates that our selective cation-exchange protocol of inorganic–organic hybrid composites is successful for producing frame-shaped nanostructures and may be developed into a generalized strategy for preparing skeleton-like nanomaterials.

Recently, semiconductor nanostructures have been found to exhibit intriguing catalytic activity for the photocatalyic hydrogen evolution from water splitting (PHWS).[18] Here, PHWS is carried out for comparative studies on the catalytic activity of hollow $Cd_{0.33}Zn_{0.67}Se$ nanoframes, hollow $Cd_{0.25}Zn_{0.75}Se$ nanoframes, and $Cd_{0.33}Zn_{0.67}Se$ nanoparticles (see Figure S6 in the Supporting Information). UV/Vis diffuse reflectance spectra (Figure 5 a) show that the spectrum of $Cd_{0.33}Zn_{0.67}Se$ nanoframes shifts to a longer wavelength relative to that of $Cd_{0.25}Zn_{0.75}Se$ nanoframes, revealing a decrease in band gap.[18b] Moreover, the absorption region of $Cd_{0.33}Zn_{0.67}Se$ nanoframes is obviously higher than that of $Cd_{0.25}Zn_{0.75}Se$ nanoframes and slightly higher than that of $Cd_{0.33}Zn_{0.67}Se$ nanoparticles, thus indicating that $Cd_{0.33}Zn_{0.67}Se$ nanoframes may exhibit the stronger absorption ability of photons over $Cd_{0.25}Zn_{0.75}Se$ frames and $Cd_{0.33}Zn_{0.67}Se$ nanoparticles. Figure 5 b shows the dependence of the H_2-evolution rate of three samples on reaction time. As displayed in Figure 5 b, the photocatalytic reaction on $Cd_{0.33}Zn_{0.67}Se$ nanoframes exhibits a stable H_2-release rate of approximately 300 μmol h^{-1} per 0.3 g of catalyst, which is about 1.5 times higher than the release rate of the reaction on $Cd_{0.25}Zn_{0.75}Se$ nanoframes. The improved activity of $Cd_{0.33}Zn_{0.67}Se$ nanoframes may be associated with their narrower band gap[18a,b] and enhanced absorption ability of photons. This improved activity also suggests that the composition of $Cd_xZn_{1-x}Se$ nanoframes has exerted a noticeable influence on their catalytic performance.[19] But, the H_2-release rate on the $Cd_{0.33}Zn_{0.67}Se$ nanoparticles decreased from 69.3 at 3 h to 33.0 μmol h^{-1} per 0.3 g of catalyst at 15 h (Figure 5 b), which is obviously lower than that of $Cd_{0.33}Zn_{0.67}Se$ nanoframes. The single-crystalline structure of the nanorods in the nanoframes could reduce the number of defects, where the photogenerated electron and hole recombine.[18a] In comparison with other solid nanostructures, the frame-shaped structures composed of nanorods could not only possess larger active surface areas and much more active sites,[18b,c] but also effectively prevent the agglomeration of catalysts. This approach may be a step forward to the preparation of novel nanoframes with optimal composition for practical H_2 production. Note that a systematic study is needed to further explore composition-dependent photocatalytic activities.

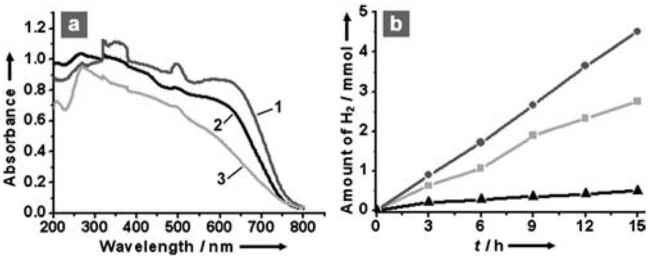

Figure 5. a) UV/Vis diffuse reflectance spectra and b) time courses of evolved H_2 under irradiation of visible-light of the as-prepared hollow $Cd_{0.33}Zn_{0.67}Se$ nanoframes (1, ●), hollow $Cd_{0.25}Zn_{0.75}Se$ nanoframes (3, ■), and $Cd_{0.33}Zn_{0.67}Se$ nanoparticles (2, ▲).

In summary, we demonstrated the successful synthesis of hollow $Cd_xZn_{1-x}Se$ nanoframes by the selective cation-exchange reaction of unpurified ZnSe–DETA hybrid nanosheets with Cd^{2+} ions. We found that the composition of $Cd_xZn_{1-x}Se$ nanoframes could be modulated by varying the ratio of the hybrid precursors to cadmium ions. The transformation mechanism from ZnSe–DETA nanosheets into hollow $Cd_xZn_{1-x}Se$ nanoframes seems to involve the selective exchange of hybrid sheets, the slow dissolution of DETA, and the subsequent Ostwald ripening process. We also showed that this selective cation-exchange strategy of hybrid nanostructures could be extended to the preparation of hollow frame-shaped metal sulfides. These hollow nanoframes are expected to be useful not only for the fundamental investigation on shape-dependent and composition-dependent optical and catalytic properties but also for many promising applications such as photocatalysis, photonics, and nanoelectonics.

Received: November 17, 2011
Revised: January 14, 2012

Keywords: cation exchange · nanoframes · nanostructures · organic–inorganic hybrid composites · photocatalysis

---

[1] a) H. G. Yang, C. H. Sun, S. Z. Qiao, J. Zou, G. Liu, S. C. Smith, H. M. Cheng, G. Q. Lu, *Nature* **2008**, *453*, 638; b) Z. Mao, R. Cartier, A. Hohl, M. Farinacci, A. Dorhoi, T. L. Nguyen, P. Mulvaney, J. Raltston, S. H. E. Kaufmann, H. Höhwald, D. Wang, *Nano Lett.* **2011**, *11*, 2152; c) C. H. Cho, C. O. Aspetti, M. E. Turk, J. M. Kikkawa, S. W. Nam, R. Agarwal, *Nat. Mater.* **2011**, *10*, 669.

[2] a) Z. Wang, D. Luan, F. Y. Chiang Boey, X. W. Lou, *J. Am. Chem. Soc.* **2011**, *133*, 4738; b) H. Zhang, H. Wang, Y. Xu, S. Zhuo, Y. Yu, B. Zhang, *Angew. Chem.* **2012**, *124*, 1488; *Angew. Chem. Int. Ed.* **2012**, *51*, 1459.

[3] a) A. W. Clark, J. M. Cooper, *Adv. Mater.* **2010**, *22*, 4025; b) C. Yan, N. Singh, P. S. Lee, *ACS Nano* **2010**, *4*, 5350; c) B. Liu, H. C. Zeng, *J. Am. Chem. Soc.* **2005**, *127*, 18262; d) T. Kouno, K. Kishino, T. Suzuki, M. Sakai, *IEEE photonics J.* **2010**, *2*, 1027; e) K. S. Cho, D. V. Talapin, W. Gaschler, C. B. Murray, *J. Am. Chem. Soc.* **2005**, *127*, 7140; f) C. Wu, H. Zhu, J. Dai, W. Yan, J. Yang, Y. Tian, S. Wei, Y. Xie, *Adv. Funct. Mater.* **2010**, *20*, 3666.

[4] a) Y. Sui, W. Fu, Y. Zeng, H. Yang, Y. Zhang, H. Chen, Y. Li, M. Li, G. Zou, *Angew. Chem.* **2010**, *122*, 4378; *Angew. Chem. Int. Ed.* **2010**, *49*, 4282; b) X. Wang, H. Fu, A. Peng, T. Zhai, Y. Ma, F. Yuan, J. Yao, *Adv. Mater.* **2009**, *21*, 1636; c) C. H. Kuo, M. H. Huang, *J. Am. Chem. Soc.* **2008**, *130*, 12815.

[5] a) D. Kim, J. Park, K. An, N. K. Yang, J. G. Park, T. Hyeon, *J. Am. Chem. Soc.* **2007**, *129*, 5812; b) A. Chen, Z. Luo, M. Akbulut, *Chem. Commun.* **2011**, *47*, 2312; c) M. A. Mahmoud, M. A. EI-Sayed, *J. Am. Chem. Soc.* **2010**, *132*, 12704; d) M. A. Mahmoud, W. Qian, M. A. EI-Sayed, *Nano Lett.* **2011**, *11*, 3285; e) X. Lu, L. Au, J. McLellan, Z. Y. Li, M. Marquez, Y. Xia, *Nano Lett.* **2007**, *7*, 1764.

[6] a) S. C. Riha, B. A. Parkinson, A. L. Prieto, *J. Am. Chem. Soc.* **2011**, *133*, 15272; b) M. D. Regulacio, M. Y. Han, *Acc. Chem. Res.* **2010**, *43*, 621; c) T. Kuykendall, P. Ulrich, S. Aloni, P. Yang, *Nat. Mater.* **2007**, *6*, 951; d) Y. Zhang, T. Mori, J. Ye, M. Antonietti, *J. Am. Chem. Soc.* **2010**, *132*, 6294; e) Y. Zhang, A. Thomas, M. Antonietti, X. Wang, *J. Am. Chem. Soc.* **2009**, *131*, 50.

[7] D. H. Son, S. M. Hughes, Y. D. Yin, A. P. Alivisatos, *Science* **2004**, *306*, 1009.

[8] a) R. D. Robinson, B. Sadtler, D. O. Demchenko, C. K. Erdonmez, L. W. Wang, A. P. Alivisatos, *Science* **2007**, *317*, 355; b) S. E. Wark, C. H. Hsia, D. H. Son, *J. Am. Chem. Soc.* **2008**, *130*, 9550; c) J. M. Luther, H. Zheng, B. Sadtler, A. P. Alivisatos, *J. Am. Chem. Soc.* **2009**, *131*, 16851; d) P. K. Jain, L. Amirav, S. Aloni, A. P. Alivisatos, *J. Am. Chem. Soc.* **2010**, *132*, 9997.

[9] a) E. Muthuswamy, S. L. Brock, *J. Am. Chem. Soc.* **2010**, *132*, 15849; b) Q. Yao, I. U. Arachchige, S. L. Brock, *J. Am. Chem. Soc.* **2009**, *131*, 2800.

[10] A. Dorn, P. Allen, D. K. Harris, M. G. Bawendi, *Nano Lett.* **2010**, *10*, 3948.

[11] B. Zhang, Y. Jung, H. S. Chung, L. van Vugt, R. Agarwal, *Nano Lett.* **2010**, *10*, 149.

[12] a) B. Sadtler, D. O. Demchenko, H. Zheng, S. M. Hughes, M. G. Merkle, U. Dahmen, L. W. Wang, A. P. Alivisatos, *J. Am. Chem. Soc.* **2009**, *131*, 5285; b) K. Miszta, D. Dorfs, A. Genovese, M. R. Kim, L. Manna, *ACS Nano* **2011**, *5*, 7176.

[13] Y. Yu, J. Zhang, X. Wu, W. Zhao, B. Zhang, *Angew. Chem.* **2012**, *124*, 921; *Angew. Chem. Int. Ed.* **2012**, *51*, 897.

[14] a) H. Li, M. Zanella, A. Genovese, M. Povia, A. Falqui, C. Giannini, L. Manna, *Nano Lett.* **2011**, *11*, 4964; b) S. Deka, K. Miszta, D. Dorfs, A. Genovese, G. Bertoni, L. Manna, *Nano Lett.* **2010**, *10*, 3770; c) K. Miszta, J. Graaf, G. Bertoni, D. Dorfs, R. Brescia, S. Marras, L. Ceseracciu, R. Cingolani, R. van Roij, M. Dijkstra, L. Manna, *Nat. Mater.* **2011**, *10*, 872.

[15] W. Yao, S. H. Yu, X. Huang, J. Jiang, L. Q. Zhao, L. Pang, J. Li, *Adv. Mater.* **2005**, *17*, 2799.

[16] a) C. M. Cobley, M. Rycenga, F. Zhou, Z. Y. Li, Y. Xia, *Angew. Chem.* **2009**, *121*, 4918; *Angew. Chem. Int. Ed.* **2009**, *48*, 4824; b) Y. Xu, H. Wang, Y. Yu, L. Tian, W. Zhao, B. Zhang, *J. Phys. Chem. C* **2011**, *115*, 15288.

[17] a) R. Li, Z. Luo, F. Papadimitrakopoulos, *J. Am. Chem. Soc.* **2006**, *128*, 6280; b) M. Saruyama, M. Kanehara, T. Teranishi, *J. Am. Chem. Soc.* **2010**, *132*, 3280.

[18] a) A. Kudo, Y. Miseki, *Chem. Soc. Rev.* **2009**, *38*, 253; b) F. Zuo, L. Wang, T. Wu, Z. Y. Zhang, D. Borchardt, P. Y. Feng, *J. Am. Chem. Soc.* **2010**, *132*, 11856; c) X. Chen, S. Chen, L. Guo, S. S. Mao, *Chem. Rev.* **2010**, *110*, 6503.

[19] S. Ouyang, J. Ye, *J. Am. Chem. Soc.* **2011**, *133*, 7757.